AIAA Guidance, Navigation, and Control Conference and Exhibit
5-8 August 2002, Monterey, California

AIAA 2002-4456

PERFORMANCE OF EVOLVED ACCELERATION GUIDANCE LOGIC FOR ENTRY (EAGLE)

J. A. Leavitt*, A. Saraf†, D. T. Chen*, and K. D. Mease‡
Department of Mechanical and Aerospace Engineering
University of California, Irvine, CA 92697

This paper presents the design and performance of Evolved Acceleration Guidance Logic for Entry (EAGLE), an algorithm intended for future space transportation vehicles. The most distinguishing feature of EAGLE is its ability to plan a three-dimensional trajectory and thereby handle large crossrange entries. EAGLE consists of two integrated components: a trajectory planner and a tracking law. The planner generates reference drag acceleration and lateral acceleration profiles, along with the reference state and bank angle profiles. The tracking law, based on feedback linearization, commands the angles of bank and attack required to follow the reference drag and heading profiles. In this paper we discuss the planner and tracking law and present simulation results indicating the performance of EAGLE. Extensive simulations of a broad range of return-from-orbit entries show that EAGLE achieves the desired target with final position and heading errors within allowable tolerances.

Introduction

The second generation of reusable launch vehicles (RLVs) under consideration in NASA's Space Launch Initiative is intended to provide a more cost-effective and capable replacement for the Space Shuttle. To achieve this goal, one area of technology development is flight mechanics. In this paper we present an entry guidance algorithm called Evolved Acceleration Guidance Logic for Entry (EAGLE) with potential to reduce the amount of pre-mission design effort, increase the range of entry opportunities, and contribute to achieving "aircraft-like" operations. EAGLE is based on the concept of planning and tracking aerodynamic acceleration profiles, a concept developed and proven effective in the Apollo and Shuttle programs. The most distinguishing feature of EAGLE relative to the Shuttle entry guidance is its ability to plan a three-dimensional trajectory, taking into account the longitudinal and lateral dimensions, and thereby handle entries as well as aborts with significant crossrange motion.

EAGLE has two integrated components: a planning algorithm which designs the entry trajectory and a tracking algorithm that generates bank angle and angle of attack commands to follow the planned trajectory. The planning algorithm constructs a drag profile based upon the total range requirement. To allow for significant lateral motion, the drag profile is constructed for the actual distance along the trajectory (in contrast to the great circle arc approximation used in the Shuttle entry planning algorithm). The bank angle variation needed to track this drag profile is also computed in the planning algorithm and used to determine the consequent lateral motion of the vehicle. Since a drag profile specifies only the magnitude of the bank angle, the sign of the bank angle is used to control crossrange. The planning algorithm determines the bank reversal required to achieve the specified crossrange.

The tracking algorithm in EAGLE implements feedback linearization based nonlinear controllers to track the drag and heading profiles generated by the planning algorithm. The bank angle command is computed as an energy dependent weighted average of the bank angles generated by the drag and heading tracking laws. The angle of attack is computed to follow a predefined angle of attack profile and also to suppress transient drag errors.

This paper presents the design and performance of EAGLE. The performance is assessed by simulating for a large number of return-from-orbit test cases. These test cases include nominal entry as well as entry with large left and right crossranges. Results obtained for dispersions in the entry conditions of these test cases are also presented.

Entry Guidance Problem

Entry Dynamics

The dynamics of atmospheric entry are expressed as a set of translational equations of motion defined in an earth-fixed coordinate frame. Since the vehicle during entry is unpowered, the energy monotonically decreases along the trajectory. Energy is an appropriate independent variable for the dynamics,[2,3] since there is no concern about the time that entry begins or ends and the target final conditions are specified at either a final velocity or final energy. With energy as the independent variable, the vehicle's translational motion can be modelled by five state equations.[3] Neglecting winds and centripetal acceleration from planet

*Graduate Research Assistant
†Postdoctoral Researcher
‡Professor; Associate Fellow AIAA

rotation, the equations of motion are[4]

$$\begin{aligned}
\theta' &= -\frac{\cos\gamma\cos\psi}{r\cos\phi}\left(\frac{1}{D}\right) \\
\phi' &= -\frac{\cos\gamma\sin\psi}{r}\left(\frac{1}{D}\right) \\
r' &= -\sin\gamma\left(\frac{1}{D}\right) \\
\psi' &= \left[\frac{\cos\psi\tan\phi}{r}\left(\frac{1}{D}\right)\right. \\
&\quad \left. + \frac{1}{V^2}\left(\frac{L\sin\sigma}{D}\right)\right]\cos\gamma + C_\psi \\
\gamma' &= \left(g - \frac{V^2}{r}\right)\frac{\cos\gamma}{V^2}\left(\frac{1}{D}\right) \\
&\quad -\frac{1}{V^2}\left(\frac{L}{D}\cos\sigma\right) + C_\gamma
\end{aligned} \tag{1}$$

where θ is the longitude, ϕ is the latitude, r is the radial distance from the vehicle's center of mass to the planet center, ψ is the heading angle with $\psi = 0$ as due east, and γ is the flight path angle. The bank angle (σ) is defined such that a bank to the right is positive and 0 bank has the lift vector directed vertically up. The lift (L) and drag (D) accelerations are given by

$$\begin{aligned}
L &= \frac{1}{2}\rho(r)V^2 \cdot \frac{S}{m} \cdot C_L(\alpha, M) \\
D &= \frac{1}{2}\rho(r)V^2 \cdot \frac{S}{m} \cdot C_D(\alpha, M)
\end{aligned} \tag{2}$$

where $\rho(r)$ is the density as a function of altitude, $C_L(\alpha, M)$ and $C_D(\alpha, M)$ are the lift and drag coefficients as functions of angle of attack α and Mach number M, S is the reference area, and m is the vehicle mass. The terms C_ψ and C_γ account for the contributions of the Coriolis acceleration due to planet rotation. These terms are given as

$$\begin{aligned}
C_\psi &= -\left(\frac{2\omega}{VD}\right)(\tan\gamma\sin\psi\cos\phi - \sin\phi) \\
C_\gamma &= -\left(\frac{2\omega}{VD}\right)\cos\psi\cos\phi
\end{aligned} \tag{3}$$

where ω is the rate of planet rotation.

A coordinate frame redefinition is used to help clarify the entry guidance problem. The coordinate frame is rotated such that the plane given by $\phi = 0$ contains both the initial and final entry positions. This rotation allows us to consider the downrange angle as θ and crossrange angle as ϕ.

Path and Control Constraints

The vehicle has maximum limits of dynamic pressure, aerodynamic acceleration, and heating rate. The limit on dynamic pressure is given by

$$Q = \frac{1}{2}\rho V^2 \leq Q_{max} \tag{4}$$

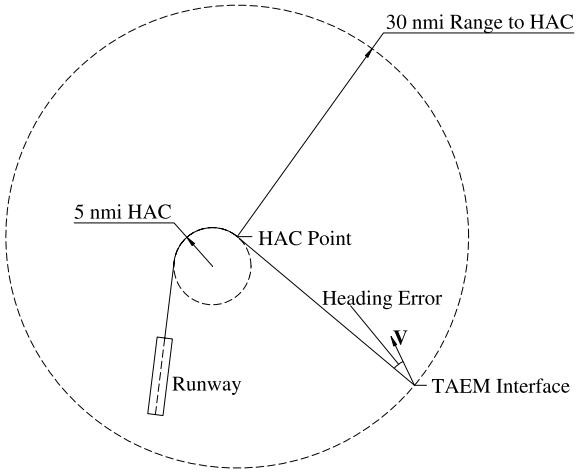

Fig. 1 Heading Alignment Maneuver During TAEM Phase.

The maximum dynamic pressure is expressed in terms of Q-alpha[5] and is constrained according to $Q_{max}\alpha = 7000$ deg-lbf/ft^2. The constraint on aerodynamic acceleration is expressed as the following constraint on normal acceleration

$$L_n = \sqrt{(L\cos\alpha)^2 + (D\sin\alpha)^2} \leq A_{max} \tag{5}$$

The maximum normal acceleration is constrained to 3.0 g. The heating rate must also not exceed the design limits of the vehicle's thermal protection. Thus, the heating rate is constrained according to the heating model

$$\dot{q} = c\rho^{1/2}V^{3.15} \leq \dot{q}_{max} \tag{6}$$

where c is a constant that is dependent on the heating model. The peak heat rate is constrained to 75 BTU/ft^2/sec.

From the guidance perspective, α and σ are treated as the controls. Both controls are restricted to be within a certain range of values and limited by rate and acceleration constraints. The value of α is constrained to remain close to a given reference angle of attack profile (α_{ref}). The value of α_{ref} starts at large angle in the beginning of the trajectory and eventually transitions down to a lower angle at the end. This type of profile is used to reduce the heat load,[1] and significant deviations from α_{ref} may increase the heat load. A limit is also placed on σ to prevent the vehicle from reaching or exceeding a 90 degree bank angle.

Entry Target Conditions

The target is determined by the desired Terminal Area Energy Management (TAEM) conditions. The TAEM point marks the beginning of the TAEM phase where the vehicle flies to a point on a Heading Alignment Circle (HAC) and performs a turn along the circle to align itself with the runway[1] (see Fig. 1). For the performance assessment described in this paper, we adopt the TAEM point conditions and error tolerances

defined for the Advanced Guidance and Control Study led by NASA Marshall Space Flight Center (MSFC).[6] The TAEM interface point is defined at a given final velocity. At this point certain state variables should be within specified error tolerances. The desired position of the TAEM point is given as 30 nmi. away from the HAC point (see Fig. 1). The maximum allowable tolerance on the final range to HAC is ±6 nmi. and the desired tolerance is ±3 nmi. The final position must also satisfy an altitude requirement of ±6000 ft. error from nominal with a desired error of ±3000 ft. A heading error is defined as the difference between the final heading and the required heading to be directed at the HAC point. The allowable heading error is ±10 degrees, but ±5 degrees is desired. The final flight path angle is restricted to be within ±4 degrees of nominal with ±2 degrees as the desired. A constraint on the final bank angle is also enforced at ±60 degrees allowable and ±50 desired.

Evolved Acceleration Guidance Logic for Entry (EAGLE)

EAGLE has evolved from the acceleration entry guidance approaches developed and used in the Apollo and Shuttle programs. The acceleration guidance concept is to plan and track aerodynamic accelerations, the rationale being that these variables can be related accurately to the planned trajectories via kinematics and measured accurately with inertial sensors. EAGLE is composed of a planning algorithm and a tracking algorithm which are described in the following subsections.

Planning Algorithm

The purpose of the planning algorithm is to determine an entry trajectory which satisfies the path constraints and target conditions. The planning algorithm is initialized with an energy dependent reference angle of attack profile, α_{ref}, and radius profile, $\hat{r}$. The equations of motion Eqs. 1 are simplified by using $\hat{r}$ to approximate r and assuming $\cos\gamma = 1$ in evaluating the state variable derivatives. The algorithm corrects $\hat{r}$ to be consistent with the planned trajectory. The freedom in the angle of attack is reserved for tracking purposes. The planning algorithm was derived by decomposing the entry trajectory planning problem into two sub-problems: a trajectory length sub-problem and a trajectory curvature sub-problem. A complete account of the entry planner can be found in Ref. [3]; the following is a summary.

Trajectory Length Sub-Problem

The trajectory length sub-problem is to determine a drag profile that satisfies the given constraints and is consistent with the required trajectory length. In the Space Shuttle entry guidance,[1] the trajectory length sub-problem is solved to obtain a feasible reference drag profile that satisfies the downrange requirement given by the great circle arc length. The drag profile is divided into segments which are quadratic with respect to velocity. This allows for an analytic solution to the range integral equation $S = -\int(V/D)dV$. Using the reference α and r profiles, the path constraints on dynamic pressure, acceleration, and heating rate (Eqs. (4)-(6)) are expressed as constraints on drag, resulting in flight corridor of allowable drag values.[1,3]

The EAGLE planning algorithm solves the trajectory length sub-problem in a similar fashion. The trajectory length is initialized as the great circle arc length to the TAEM point. Treating energy as the independent variable, the range integral equation becomes $S = -\int(1/D)dE$. The current prototype uses a three segment linear spline reference drag profile with additional constraint arcs if needed to satisfy the path constraints. With a curved trajectory, the required trajectory length S will be longer than the downrange given by

$$R = -\int \frac{\cos\psi}{D\cos\phi} dE \tag{7}$$

To correct the value of S a corresponding solution to the trajectory curvature sub-problem must be determined.

Trajectory Curvature Sub-Problem

The trajectory curvature sub-problem is to determine a lateral acceleration profile that is consistent with the drag profile given by the trajectory length sub-problem and that meets the desired final crossrange. The lateral acceleration from a given drag profile can be determined by differentiating drag twice to obtain

$$\frac{L}{D}\cos\sigma = \frac{1}{b}(D'' - a) \tag{8}$$

where

$$\begin{aligned} a &= D\left(\frac{C_D''}{C_D} - \frac{C_D'^2}{C_D^2}\right) + D'\left(\frac{C_D'}{C_D} + \frac{2}{V^2}\right) \\ &\quad -\frac{4D}{V^4} + \frac{1}{DV^2}\left(\frac{1}{h_s} + \frac{2g}{V^2}\right)\left(g - \frac{V^2}{r}\right) \\ &\quad + \left(\frac{1}{h_s} + \frac{2g}{V^2}\right) C_\gamma \\ b &= -\frac{1}{V^2}\left(\frac{1}{h_s} + \frac{2g}{V^2}\right) \end{aligned} \tag{9}$$

Using the reference angle of attack profile, the lateral acceleration can be computed by

$$|L\sin\sigma| = D\left[\left(\frac{L}{D}\right)^2 - \left(\frac{L}{D}\cos\sigma\right)^2\right]^{1/2} \tag{10}$$

Thus the drag profile only determines the magnitude of the lateral acceleration and the bank direction remains free for changing the heading and crossrange profiles. The bank direction is determined in the planning algorithm by integrating the differential equations

for heading and crossrange (ψ' and ϕ' in Eqs. (1)) and performing a search for the required bank reversal to minimize the final error. The point at which the reversal occurs determines the amount of time that the vehicle spends banked in the right (+) and left (-) directions which effects the trajectory curvature. The "bank reversal time" is the parameter which is adjusted by the planning algorithm to determine the trajectory curvature and satisfy the constraint on the final crossrange. The bank rate and acceleration limits are respected in the above process.

Successive Approximation Procedure

Since the intent of the EAGLE planning algorithm is to accommodate entries and aborts with significant crossrange, the assumption that the downrange (i.e., the great circle distance) to the target is a sufficiently accurate estimate of trajectory length is not appropriate. With the crossrange profile, it is possible to integrate Eq. (7) and the trajectory length estimate. The following iterative process is used to successively improve the trajectory length and curvature estimates.

1. Estimate the trajectory length and solve the trajectory length sub-problem to obtain an initial drag profile.
2. Using the current estimate of the drag profile, solve the trajectory curvature sub-problem.
3. Based on the solution to the trajectory curvature sub-problem, adjust the trajectory length by $S_{i+1} = S_i + (S_0 - R_i)$, where i is the iteration index, and solve the trajectory length sub-problem to obtain a revised drag profile.
4. If the target error is sufficiently small, stop; otherwise, repeat Steps 2-4.

This procedure will generate reference drag and heading profiles and a reference bank command that the tracking law will operate on. To compensate for tracking errors, the reference trajectory is updated at various times along the trajectory. At each update the reference trajectory is replanned from the vehicle's current position using the same successive approximation, except that the estimated parameters are initialized from the previously planned trajectory.

Bank Reversal Management

The prototype EAGLE algorithm plans a fixed number of bank reversals. After the vehicle has performed its last bank reversal, the reference heading profile is not updated. If the remaining distance to the target is too large, an unacceptable crossrange error could result. To avoid this problem, it is desirable the final bank reversal occur close to the target. For short trajectories a single bank reversal may be adequate, whether it be early or late in the entry phase. For longer cases, however, the planning of more than one bank reversal may be necessary, with the last reversal constrained to occur within a certain distance from the TAEM interface point. To deal with the return-from-orbit cases considered in the Results section, a two-reversal approach was implemented using the one-reversal planner. First the planner determines a single-reversal trajectory. However, the reversal is actually executed slightly earlier than planned. This creates the need for a second, corrective bank reversal near the end of the entry phase. The second reversal is then planned and executed as normal.

For high crossrange cases, a trajectory that is initially turning toward the target will have the first and second bank reversals occurring close to the end of the trajectory. If the vehicle is initially turning away from the target, the first bank reversal will occur earlier in the trajectory. Because of the negative impact on drag tracking, it is not desirable to perform the two reversals close to each other. The prototype planning algorithm solves this problem by initially turning the vehicle away from the target in these cases; this however would not be a good strategy near the maximum crossrange boundary.

Meeting the Final Heading Constraint

As stated previously, the constraint on final heading angle is that the vehicle be headed toward the HAC point when it reaches the TAEM interface circle. Because the planner only determines one bank reversal in a trajectory update, the final heading cannot be specified. Instead, the freedom to select the location of the TAEM point has been used to meet the heading constraint. If the location of the TAEM point at the desired range to HAC does not significantly affect the planned final heading, the following selection method can be used during planning updates. First, plan the trajectory using the current approximation of the TAEM point location. Next, determine the final velocity vector from the planned trajectory. Finally, relocate the TAEM point along the desired range to HAC circle so that the velocity vector aligns with the HAC point. Do this at each planning update that occurs after the first reversal and before the second. If the second bank reversal is planned too close to the desired range to HAC, the final heading angle can change significantly with changes in TAEM point location. As a result, the TAEM point search may not converge. In the prototype algorithm, this problem is solved by halving the TAEM point movement at each iteration, if the final reversal is close to the target.

Tracking Algorithm

EAGLE uses bank angle as the primary control variable and angle of attack as the secondary control variable to track the reference trajectory generated by the planning algorithm. In the Shuttle guidance, bank angle is commanded to track the drag reference profile only. The tracking algorithm in EAGLE com-

mands the bank angle to follow both drag and heading reference profiles. The angle of attack in EAGLE is modulated about the given reference profile to correct only the transient drag errors.

The bank angle command is derived by first treating $u_1 = (L/D)\cos\sigma$ and $u_2 = (L/D)\sin\sigma$ as two independent inputs. Defining drag and heading as outputs of the system dynamics and u_1, u_2 as inputs, the following equations can be obtained:

$$\begin{aligned} D'' &= a + bu_1 \\ \psi' &= \frac{\cos\gamma\cos\psi\tan\phi}{rD} + \frac{1}{V^2\cos\gamma}u_2 + C_\psi \end{aligned} \tag{11}$$

where a and b are as defined in Eqs. (9). Thus u_1 and u_2 can be used to linearize the drag dynamics and the heading dynamics respectively. In fact, u_1 can be computed so that drag tracks the reference drag profile according to specified second order linear error dynamics. Letting D_r represents the reference drag and D_r' and D_r'' represent the derivative of reference drag with respect to energy, the specified second order linear error dynamics are

$$\begin{aligned} (D_r'' - D'') + k_p(D_r - D) + \\ k_d(D_r' - D') + k_i\textstyle\int(D_r - D)dE \end{aligned} \quad = \quad 0 \tag{12}$$

Here k_p, k_i and k_d are the proportional, integral and derivative gain constants respectively. Substituting for D'' from Eq. (11), the input u_1 required to track D_r is given by

$$\begin{aligned} u_1 \quad = \quad & \tfrac{1}{b}[-a + D_r'' + k_p(D_r - D) + \\ & k_d(D_r' - D') + k_i\textstyle\int(D_r - D)dE] \end{aligned} \tag{13}$$

Similarly, u_2 can be computed so that heading tracks the reference heading profile according to the first order error dynamics

$$(\psi_r' - \psi') + k_1(\psi_r - \psi) + k_2\int(\psi_r - \psi)dE = 0 \tag{14}$$

where ψ_r represents the reference heading, ψ_r' the first derivative of heading with respect to energy and k_1 and k_2 are the proportional and integral gains. Substituting for ψ' from Eqs. (1) we get

$$\begin{aligned} u_2 \;=\; V^2\cos\gamma\Bigg[& -\frac{\cos\gamma\cos\psi\tan\phi}{rD} - C_\psi \\ & + \psi_r' + k_1(\psi_r - \psi) + k_2\int(\psi_r - \psi)dE\Bigg] \end{aligned} \tag{15}$$

corresponding bank angles can now be computed from both u_1 and u_2 using measured L and D and the definitions

$$\sigma_D = \cos^{-1}\left(\frac{Du_1}{L}\right) \tag{16}$$

and

$$\sigma_\psi = \sin^{-1}\left(\frac{Du_2}{L}\right) \tag{17}$$

As can be seen, σ_D can assume either a positive or a negative sign. For drag tracking, only the magnitude of bank angle is important. However, the sign of the bank angle and reversals of sign are important for accurate crossranging. The sign of σ_D is therefore set equal to the sign of the reference bank angle data (σ_{ref}) generated by the planning algorithm.

The commanded bank angle σ_{cmd} is calculated as the following weighted average of σ_D and σ_ψ

$$\sigma_{cmd} = w(E)\mathrm{sgn}(\sigma_{ref})\sigma_D + (1 - w(E))\sigma_\psi \tag{18}$$

where $w(E)$ is a continuous function of energy and takes values between 0 and 1. In the initial portion of the entry, $w(E)$ takes a value 1 and emphasizes drag tracking completely. In the latter portion w is chosen to take a value of about 0.6-0.7. Drag tracking is emphasized initially because drag tracking is quite challenging by itself and requires full attention; if drag is tracked accurately, then nominally the reference heading will be followed. Moreover, at each planning update, a reference profile starting from the current heading is designed and hence the heading error is nullified.

The gains used in the computation of u_1 are scheduled as functions of dynamic pressure. The following function is used for scheduling:

$$2\left(\frac{Q}{Q_{max}}\right) - \left(\frac{Q}{Q_{max}}\right)^2 \tag{19}$$

This function directly multiplies the natural frequency of the error dynamics and the integral gain. The natural frequency and the integral gain are kept small in the initial part of the trajectory where dynamic pressure is low. This is to ensure that the bank angle does not become saturated in response to small drag errors in low dynamic pressure conditions. Since the bank rate limited to 5 deg/sec, the prevention of bank angle saturation makes it more likely that the appropriate bank angles can be achieved as the dynamic pressure and drag increase.

The angle of attack command primarily follows the reference profile that is used by the planning algorithm to generate the drag and heading profiles. However, angle of attack is also modulated to reduce the transient errors in drag tracking. To achieve this the drag error is converted to an angle of attack adjustment, using the coefficient of drag and Q and then passed through the washout filter $s/(s+0.002)$. This angle of attack adjustment is limited to ± 5 deg. and added to the reference value. The bank angle and angle of attack commands are rate limited to ± 5 deg/sec so as to be consistent with the vehicle capability as modelled in this paper.

Results

This section presents the performance of EAGLE as implemented in the Marshall Aerospace Vehicle Rep-

Case	EG13	EG14	EG15
Initial Height (m)	121518.	122558.	120374.
Latitude (deg)	-18.255	-22.510	-12.223
Longitude (deg)	-117.01	-111.01	-125.01
Initial Vel. (m/s)	7622.0	7621.3	7622.79
Initial Hdg. (deg)	38.329	39.856	36.812
HAC Lat. (deg)	28.6112	28.6112	28.6112
HAC Long. (deg)	-80.496	-80.496	-80.496
TAEM Alt. (ft)	99827.3	99827.3	99827.3
TAEM Vel. (ft/s)	2979.0	2979.0	2979.0

Case	EG16	EG17	EG18
Initial Height (m)	121859.	123104.	120132.
Latitude (deg)	-29.516	-33.263	-23.751
Longitude (deg)	-127.50	-122.50	-134.50
Initial Vel. (m/s)	7625.99	7625.15	7627.18
Initial Hdg. (deg)	43.447	46.06	40.409
HAC Lat. (deg)	28.67	28.67	28.67
HAC Long. (deg)	-80.506	-80.506	-80.506
TAEM Alt. (ft)	96560.0	96560.0	96560.0
TAEM Vel. (ft/s)	3008.08	3008.08	3008.08

Case	EG19	EG20	EG21
Initial Height (m)	121650.	122079.	124848.
Latitude (deg)	-2.3046	-8.446	22.83
Longitude (deg)	-141.72	-137.72	-157.72
Initial Vel. (m/s)	7442.37	7442.07	7440.12
Initial Hdg. (deg)	59.854	61.026	71.4535
HAC Lat. (deg)	28.6112	28.6112	28.6112
HAC Long. (deg)	-80.496	-80.496	-80.496
TAEM Alt. (ft)	99827.3	99827.3	99827.3
TAEM Vel. (ft/s)	3008.08	3008.08	3008.08

Table 1 Initial and Target Conditions

resentation In C (MAVERIC) simulation environment. The vehicle model used in the test cases is representative of the X-33.[7] The test cases presented for demonstrating the performance of EAGLE are named EG13 to EG21 (EG denoting Entry Guidance) and defined by NASA MSFC.[6] All of these are return-from-orbit test cases and a summary of the initial and desired target (TAEM point) conditions are presented in Table 1. The initial conditions correspond to the beginning of the transition phase of flight. The initial conditions for entry are obtained by integrating the vehicle dynamics to the end of the transition phase.

Fig. 2 shows some key variables for the simulated entry using the EAGLE algorithm for the EG17 case. The variables are plotted against the normalized total energy $\tilde{E} = (E - E_i)/(E_f - E_i)$, where E is the current energy, E_i and E_f are the initial and the desired final energy values respectively. With this formulation $\tilde{E} = 0$ at the start of the entry phase and reaches a value of 1 at the nominal TAEM condition. The planner generates reference heading and drag profiles and updates these profiles every 60 or 80 sec. The planner also generates a reference bank angle profile which is consistent with the drag and heading profiles. These reference profiles are plotted in Fig. 2 along with the actual drag, heading angle, and the commanded bank angle and angle of attack. It can be seen that the heading and drag reference profiles are tracked quite well. Two bank reversals can be identified at the normalized energies of 0.12 and 0.95. As explained in the Planning Algorithm subsection, the two reversals are actually obtained by advancing the first reversal by about $\tilde{E} = 0.035$ and then planning the second reversal after the first reversal is completed. The second reversal usually occurs beyond $\tilde{E} = 0.92$. Slight errors in drag tracking take place when a bank reversal is commanded and when drag reference profile has corners at $\tilde{E} = 1/3$ and $\tilde{E} = 2/3$. Angle of attack normally follows the reference value and responds only to transient errors in drag tracking. Such a response in angle of attack has been obtained by using a washout filter in the feedback path as explained in the Tracking Algorithm section.

Fig. 3 shows the ground tracks of the trajectories EG13 to EG15 and Fig. 4 shows ground tracks for the cases EG16-EG21. In EG13, EG16 and EG19, the vehicle is headed directly toward the HAC point at entry. The remaining cases have significant right and left crossrange offsets. All the cases have significant lateral motion and EAGLE uses the two bank reversals effectively to reach the TAEM point with minimal downrange, crossrange and heading errors. Also plotted in Fig. 3 and 4 are the variations in initial latitude and longitude for each case considered in this paper. These variations are caused by X, Y, Z position dispersions of the transition point by ± 33 m and velocity dispersions at the transition point by ± 0.33 m/s. Each of these dispersions is taken one at a time along each axis.

Fig. 5 and 6 show a close up around the HAC point. Each simulation is terminated when the vehicle velocity becomes equal to the TAEM velocity given in Table 1. It is desired that at the TAEM velocity, the vehicle should be within 27-33 nmi. from the HAC point, within ± 3000 ft. of TAEM altitude (mentioned in Table 1) and within ± 5 deg. of heading towards the HAC point, but errors twice this size are considered allowable. Fig. 5 and 6 show a portion of the 30 nmi. circle around the HAC point and the tolerable band of ± 3 nmi. Also plotted are the final segments of EG13-21 nominal cases and the end-points of all the dispersion cases considered. The end-points of all the trajectories lie within the ± 3 nmi. band. The nominal trajectories also appear to head correctly towards the HAC points.

The actual heading errors and altitude errors (relative to the TAEM altitude in Table 1) are plotted in Fig. 7 and 8 respectively. In these plots dispersions in the position and velocities along X, Y, and Z axes are indicated along the abscissa. It can be seen from

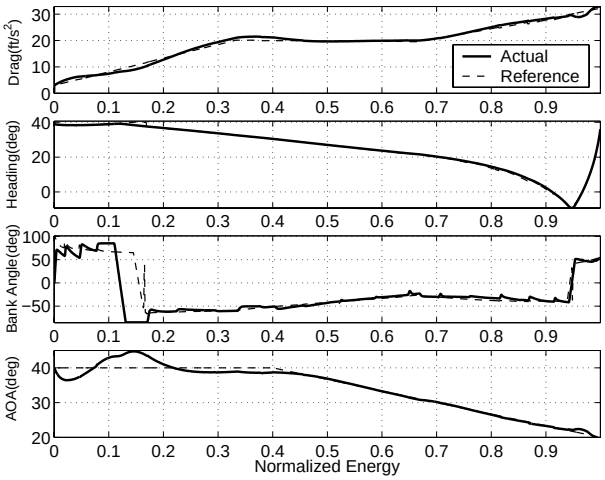

Fig. 2 Trajectory Profiles for EG17

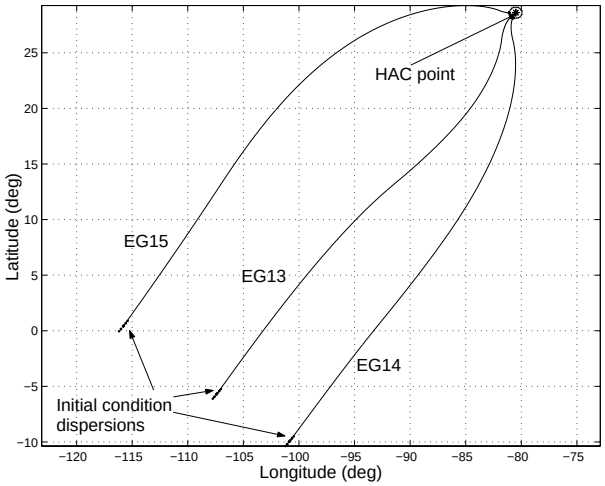

Fig. 3 Ground Track for EG13 to EG15.

Fig. 7 that very few cases exceed the 5 deg. band of heading error and only one case exceeds the 3000 ft. altitude error in Fig. 8. All the results fall within the allowable range of error.

Conclusions

A prototype entry guidance algorithm, called EAGLE (Evolved Acceleration Guidance Logic for Entry), has been described and its performance has been assessed for 9 return-from-orbit cases using the MAVERIC simulation. For each case, 12 additional initial condition dispersions have been simulated. The results of these simulations show that EAGLE achieves the desired targeting accuracy for most all the cases and achieves the allowable accuracy for all the cases. In particular the large crossrange trajectories (EG14, EG15, EG17, EG18, EG20 and EG21) are successfully handled by EAGLE.

Acknowledgment

This research was funded by NASA Marshall Space Flight Center and by Universal Space Lines, LLC.

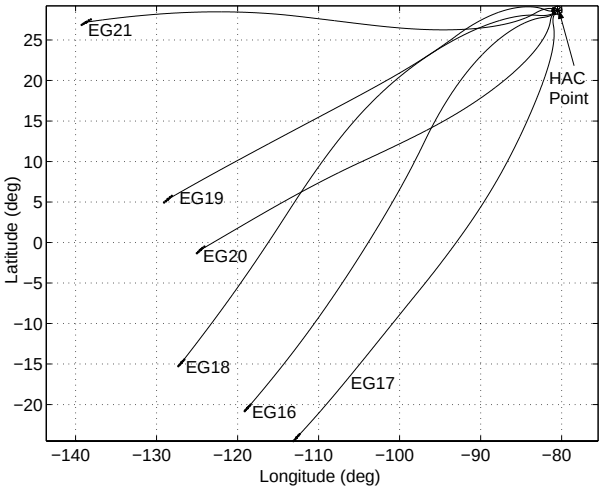

Fig. 4 Ground Track for EG16 to EG21.

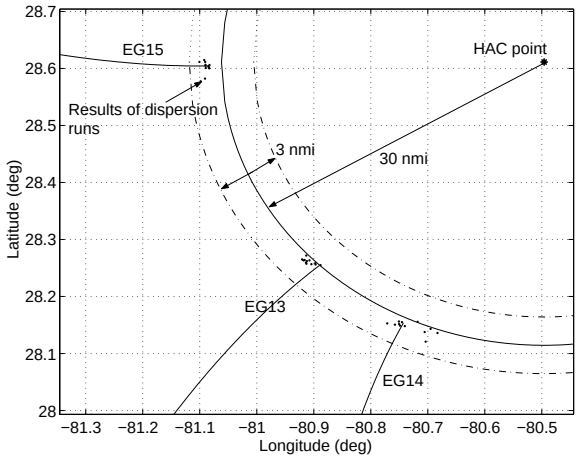

Fig. 5 TAEM Point Dispersions for EG13 to EG15.

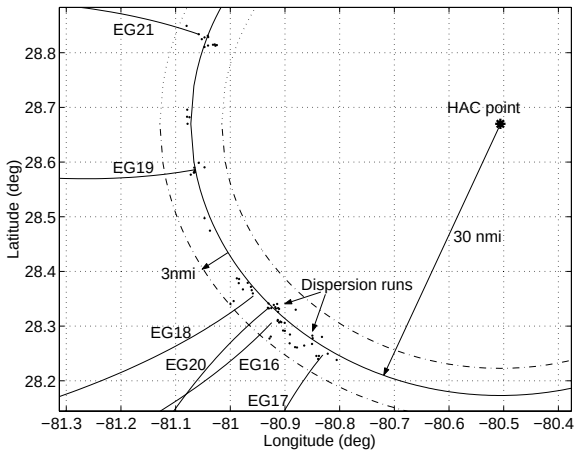

Fig. 6 TAEM Point Dispersions for EG16 to EG21.

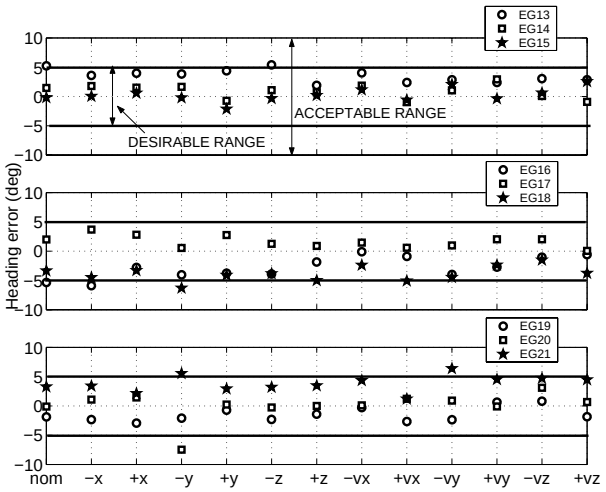

Fig. 7 Final Heading Error.

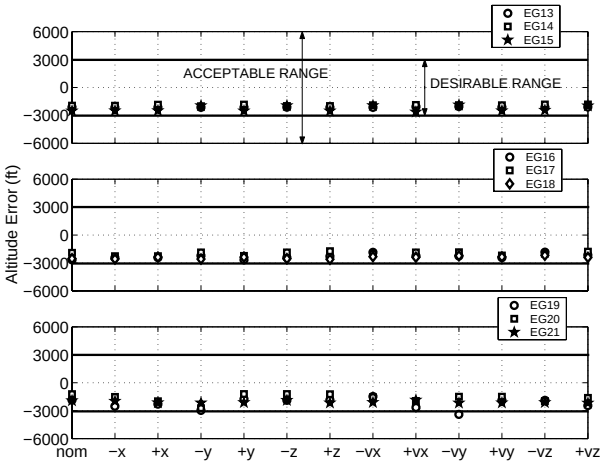

Fig. 8 Final Altitude Error.

References

[1]Harpold, J.D., and Graves, C.A., Jr., "Shuttle Entry Guidance," *J. Astronautical Sciences*, Vol. 27, No. 3, 1979, pp. 239-268.

[2]Stengel, R.F., "Optimal Guidance for the Space Shuttle Transition," *J. Spacecraft*, Vol. 11, No. 3, 1974, pp. 173-179.

[3]Mease, K.D., Chen, D.T., Teufel, P., and Schönenberger, H., "Reduced-Order Entry Trajectory Planning for Acceleration Guidance," *J. Guidance, Control, and Dynamics*, Vol. 25, No. 2, 2002, pp. 257-266.

[4]Vinh, N.X. *Optimal Trajectories in Atmospheric Flight*, Elsevier, New York, 1981.

[5]Hill, A.D., Anderson, D.M., Coughlin, D. J., and Chowdhry, R. S., "X-33 Trajectory Optimization and Design," Paper 98-4408, AIAA GNC-Conference, Boston, Aug. 1998.

[6]Hanson, J., Jones, R., and Krupp, D., "Advanced Guidance and Control Methods for Reusable Launch Vehicles: Test Results," Paper 2002-4561, AIAA GNC-Conference, Monterey, Aug. 2002.

[7]Hanson, J.M., Coughlin, D.J., Dukeman, G.A., Mulqueen, J.A., and McCarter, J.W., "Ascent, Transition, Entry, and Abort Guidance Algorithm Design for the X-33 Vehicle," Paper 98-4409, AIAA GNC-Conference, Boston, Aug. 1998.